論文 / 著書情報
Article / Book Information

Title	Droplet-based valveless microfluidic system for phage-display screening against spheroids
Authors	Tsuyohi Sato, Akira Hamai, Tetsuya Kadonosono, Shinae Kizaka-Kondoh, Toru Omata
Citation	Biomicrofluidics, Volume 16, Issue 2,
Pub. date	2022, 4
Note	This article may be downloaded for personal use only. Any other use requires prior permission of the author and AIP Publishing. This article appeared in Biomicrofluidics, Volume 16, Issue 2, and may be found at https://doi.org/10.1063/5.0085459.

Droplet-based valveless microfluidic system for phage-display screening against spheroids

Tsuyohi Sato[1], Akira Hamai[1], Tetsuya Kadonosono[2], Shinae Kizaka-Kondoh[2] and Toru Omata[1,a]

AFFILIATIONS
[1]Dept. of Mechanical Engineering, Tokyo Institute of Technology, 226-8503 Kanagawa, Japan
[2]Dept. of Life Science and Technology, Tokyo Institute of Technology, 226-8503 Kanagawa, Japan
[a]Author to whom correspondence should be addressed: omata.t.aa@m.titech.ac.jp

ABSTRACT

In this study, we proposed a droplet-based valveless microfluidic system that has the necessary functions to perform the binding, washing, eluting, and collecting processes of phage-display screening against spheroids, which can be expected to present a similar repertoire and number of membrane proteins as *in vivo*. Although spheroids have much larger sizes than single cells, spheroids are difficult to manipulate through manual operation. The proposed microfluidic system actively controls the position and velocity of droplets using a camera, three air pumps, and three liquid pumps to perform the processes for phage-display screening. The cross-section of the microchannel is large in width and height for the passage of spheroids. Valves that can close such a large cross-sectional microchannel are not readily available. Thus, we proposed valveless flow control using liquid pumps. In addition, the proposed microfluidic system involves complex flow channels with airflow subchannels to perform phage-display screening. For washing, nonspecific-binding phages remaining in the flow channels must be minimized. The proposed microfluidic system can perform selective blocking and flush washing. Selective blocking can prevent the airflow channels from becoming hydrophilic with blocking liquid, and flush washing can flush phages remaining in the flow channel. We experimentally verified the functions of the developed microfluidic device based on the proposed system.

I. Introduction

Phage display can display proteins or peptides on the surface of phages by gene recombination, and phage-display screening is a robust method for identifying specific binding proteins or peptides of target molecules[1,2] from artificially produced libraries that include millions of them with different amino acid sequences. Phage-display screening involves binding, washing, eluting/collecting, amplifying, and identifying processes. The biding process incubates phage library with target molecules to allow their specific binding; the washing process washes target molecules to remove unbound and nonspecific-binding phages; the eluting/collecting process detaches the binding phages from the target molecules with an eluent and collects the phages; the amplifying process amplifies the collected phages by infecting them with bacteria, such as *Escherichia coli*. The amplified phages are used as libraries in the next round of processes, which are repeated 3–6 times. The amplified phages in the last round are genetically analyzed for specific binding peptides identification.

The conformation of target molecules in phage-display screening should be the same as *in vivo*. The characteristics of target molecules may change in different three-dimensional (3D) conformations, even when the amino acid sequences are the same. The conformations of membrane proteins are not maintained without cell surface membranes[3-5]. To avoid this problem, cell-based phage-display screening is promising[6]. For efficient execution of the processes of cell-based phage-display screening, a precise, stable, and uniform flow control toward cells is required. Microfluidic flow control is suitable; moreover, microfluidic devices for phage-display screening against monolayer cultured and suspended cells have been proposed[7-9].

However, the repertoire and numbers of membrane proteins expressed on suspended single cells and monolayer-cultured cells differ from *in vivo* tissues. Therefore, 3D cultured cells, such as spheroids[10,11], which can be expected to present a similar repertoire and number of membrane proteins as *in vivo*, are preferable. Although spheroids have much larger sizes than single cells, spheroids are difficult to manipulate through manual operation and many studies have employed a microfluidic device for the spheroid formation and culture[12]. In this study, we propose a microfluidic system that has the necessary functions to perform the binding, washing, eluting, and collecting processes of phage-display screening against spheroids[13-15]. The system is based on droplet flow control[16-18] because droplet-based flow control can easily perform spheroid transportation to the succeeding process in phage-display screening. In addition, the internal flow of a droplet during transportation is advantageous for binding and washing phages.

Many droplet-based microfluidic devices employ passive control of droplets[19] by pushing droplets in built-in microfluidic components in order. However, passive control is not always stable and has limitations. Meanwhile, active droplet control is suitable for complex operations[20]. The active droplet control in a simple microchannel[21] realizes the forming, splitting, merging, mixing, and sorting of droplets with approximately ±10% error. Although active droplet

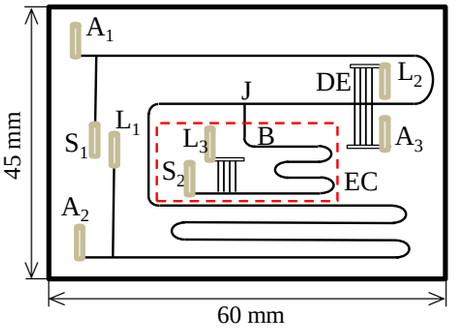

FIG. 1. Proposed microfluidic system. S_1 and S_2: manual syringes, A_1, A_2, and A_3: air pumps, L_1, L_2, and L_3: liquid pumps, DE: drainage/exhaust region, EC: eluting/collecting region, J: junction of the main and branch flow channels, B: branch flow channel.

control requires sensors and actuators, their cost has been reduced recently.

The proposed microfluidic system employs a camera, three air pumps, and three liquid pumps. We show that it can perform the functions of phage-display screening processes by actively controlling the position and velocity of a droplet with visual feedback. The cross-section of microchannels is large in width and height for the passage of spheroids. Valves that can close such large cross-sectional microchannels are not readily available, except for a recently developed one[22]. Valve function is necessary to implement a branch flow channel for the eluting/collecting process. We propose a valveless flow control using the liquid pumps.

For washing, nonspecific-binding phages remaining in the flow channels must be minimized. The proposed microfluidic system involves complex flow channels with airflow subchannels to perform phage-display screening. The proposed microfluidic system can perform selective blocking that can prevent the airflow subchannels from being hydrophilic with the blocking liquid as well as flush washing that can flush phages remaining in the flow channel. We experimentally verify the functions of the developed microfluidic device based on the proposed system, which is a necessary step toward phage-display screening against spheroids.

II. Method

A. Microfluidic system overview

Fig. 1 shows the proposed microfluidic system comprising two manual syringes (S_1 and S_2), three liquid pumps (L_1, L_2, and L_3), and three air pumps (A_1, A_2, and A_3). DE is the drainage/exhaust region. The design values of the height and width of the flow channel are 350 and 500 µm, respectively, assuming that a spheroid of approximately 300-µm diameter is introduced. Several flow subchannels are connected to DE from both sides to drain liquid with L_2 and exhaust air with A_3 without sucking a spheroid. The height and width of the flow subchannels are 50 and 200 µm, respectively. The length of the DE region is 1250 µm. EC is the eluting/collecting region. B is the branch flow channel, and J is the junction of the main and branch flow channels.

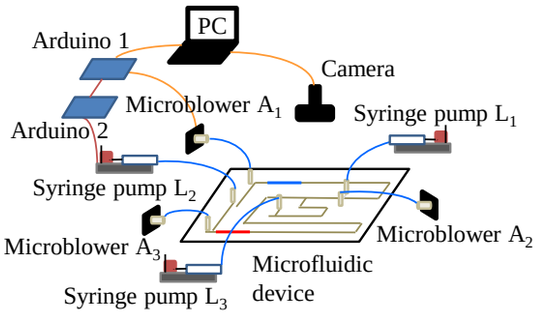

FIG. 2. System hardware[14]. Arduinos 1 and 2 control the microblowers and syringe pumps, respectively. Some electric cables connecting the arduinos are omitted. Manual syringes S_1 and S_2 are also omitted

To ensure that no spheroids are sucked from B, L_3 is connected to B through several flow subchannels. The developed microfluidic device had two flow channels with different heights of 50 and 350 µm, and its fabrication process employed two-step exposure (see the Supplementary Material for the fabrication details).

B. System hardware

Fig. 2 shows the hardware of the system. Syringe pumps are applied as liquid pumps L_1, L_2, and L_3. Custom-made syringe pumps were assembled using a commercial ball-screw device (One-axis actuator, LS, Misumi Corporation, stroke: 140 mm, lead: 2 mm) and stepping motor (ST-42BYH1004, step: 400) microblower (Murata Inc. MZB1001T02) were used as A_1, A_2, and A_3. The microblower is a compact and inexpensive air pump, preventing the increase of the device size and cost. It drives air using pulse width modulation (PWM)-controlled ultrasonic ceramic vibration. Owing to the PWM control, the output airflow was not constant. To solve this problem, we increased the length of the silicon tube connecting the microblower and microfluidic device to 900 mm.

An industrial camera (DFK33UP1300, Imaging Source) with background lighting was employed to detect the droplet and measure its position and velocity. The resolution (480 × 640 pixels) was selected by considering the flame rate of 30 frame/s. One pixel corresponded to approximately 62.5 × 62.5 µm. This low resolution was permitted because functions were separately arranged in the device and a large error of 200 µm was permitted for droplet position measurement. Arduinos 1 and 2 control the microblowers and syringe pumps, respectively. The two arduinos were connected to a PC, which processed the images taken by the camera with MATLAB.

C. Branch control

In the binding and washing processes, the spheroid droplet must not enter B. Thus, L_3 introduces an eluate droplet in B and makes the air volume between the spheroid and eluate droplets small [Fig. 3(a)]. Actually, the spheroid droplet enters B partially. However, if the entered volume is

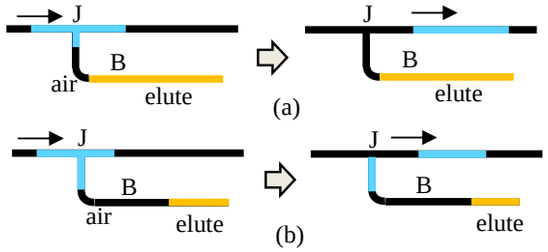

FIG. 3. Branch control: (a) little air volume between two droplets and (b) large air volume; a part of droplet remains in B.

little, it is brought out of the branch by the main volume of the spheroid droplet due to the liquid intermolecular force. The air spring constant is given by

$$K_a = \gamma A^2 P/V$$

where γ is the ratio of specific heat, A is the area of the cross-section of B, whereas P and V are the pressure and volume of air, respectively. When the adiabatic expansion is assumed, we have PV^{γ} = const and

$$K_a \propto \gamma A^2/V^{1+\gamma}$$

Therefore, K_a can be made large by making the air volume little, which can prevent the spheroid droplet from entering B.

D. Operation of the binding and washing processes

Fig. 4 depicts the operation of the biding and washing processes comprising eight steps (EC is omitted). The eight steps in Fig. 4 are performed as follows.

Binding Process:

- Step 1 introduces a droplet containing a spheroid (spheroid droplet for short) and phages using syringe S_1. As this is done only once, a manual syringe is used
- Step 2 moves the droplet toward DE with the air pressure supplied by A_1

Note: When a droplet moves in a microchannel, an internal circulating flow occurs and its velocity can be controlled by the droplet velocity[13]. Step 2 moves a spheroid droplet with a relatively slow speed not to remove the specific binding phages on the spheroid. The internal flow is even expected to promote contact between specific binding phages and spheroid cells when its velocity is small, and step 2 can be extended arbitrarily by moving the droplet to the zigzag flow channel, reciprocating it there and moving it back to DE.

Washing process:

This process comprises subprocesses: drainage (step 3), flush (step 4), merge (steps 5 and 6), and mixture (step 7).

- Step 3 drains the droplet liquid at DE by applying negative pressure via L_2 until the droplet reaches a predetermined volume. In the first round, skip step 4 and go to step 5.
- Step 4 flushes the flow channel with washing liquid [phosphate-buffered saline(PBS)] to remove phages remaining in the flow channel. The washing liquid is introduced via L_1 and drained via L_2.
- Step 5 also introduces the diluent solution (PBS) into the flow channel via L_1, which is then cut to form a droplet and moved to DE by applying air pressure via A_2. The droplet of PBS moves the spheroid droplet to the right due to the increase of the air pressure between them. The spheroid droplet stops on the right of DE because air exhausts from the flow subchannels. For the air exhaust, A_3 is set off.
- Step 6 moves the spheroid droplet to the left for merging with the diluent solution droplet and moves the merged droplet to the zigzag flow channel via A_1.
- Step 7 reciprocates the merged droplet to mix the liquid in it using the internal flow, via A_1 and A_2, alternatively. When A_1 moves the droplet with its air pressure, A_3 is switched on such that the air does not escape from the flow channel, whereas when A_2 moves the droplet, it is switched off. This step moves the droplet with a higher speed, which is expected to increase the speed of the internal flow and wash out the low-specific binding phages on the spheroid cells.
- Step 8 moves the droplet to DE via A_2 and performs step 3.

Then, steps 4–8 are repeated as many times as needed.

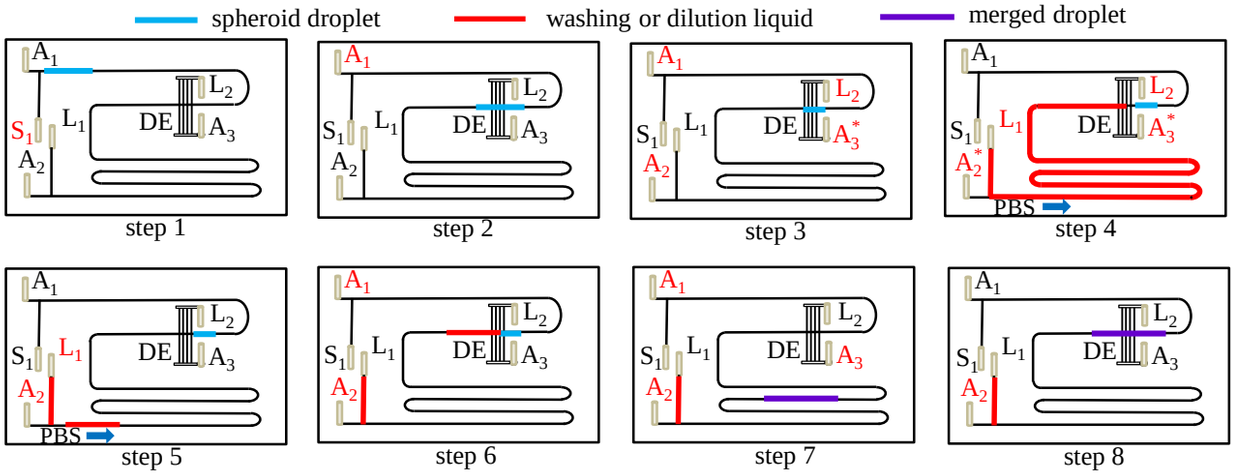

FIG. 4. The binding (steps 1 and 2) and washing processes (steps 3–8). On pumps are colored red. Air pump A_i (i = 2 and 3) with superscript * is on to prevent liquid from entering the flow channel connected to it. Step 1: introduction of a spheroid droplet from S_1, Step 2: movement to DE via A_1, Step 3: drainage from L_2, ($A_1$and A_2 are on to maintain the position of the spheroid droplet at DE.), Step 4: flushing of washing liquid from L_1, Step 5: introduction of a droplet of dilution solution from L_1, Step 6: merging of the two droplets, Step 7: reciprocation of the merged droplet for mixing (A_1 and A_2 are switched on alternatively. When A_1 is on, A_3 is also on.), and Step 8: movement to DE via A_2 then return to Step 3.

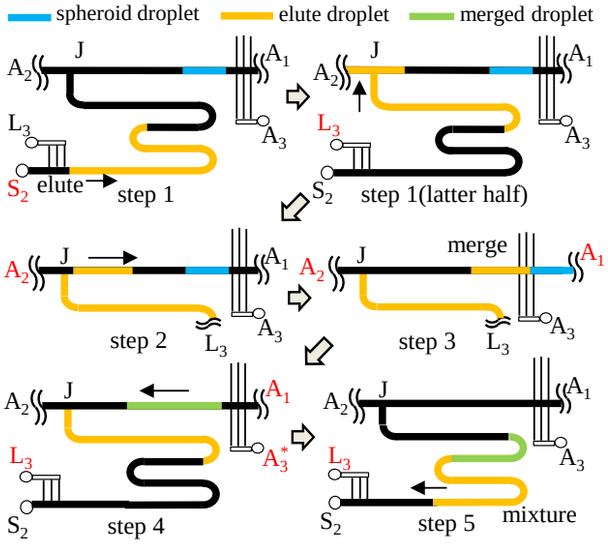

FIG. 5. The eluting/collecting process. On pumps are colored red. Step 1: introduction of an elute solution from S_2 and movement to the main channel, Step 2: cutting off the elute solution to form a droplet via A_2, Step 3: merging of the two droplets, Step 4: movement to J, Step 5: collection of the merged droplet via L_3.

E. Operation of the eluting/collecting process

Fig. 5 depicts the operation of the eluting/collecting process comprising five steps. This process uses L_3.
- Step 1: The eluate is manually introduced with S_2 and is moved to the main channel through J under the air pressure applied by L_3. In this step, L_3 is used as an air pump.
- Step 2 The eluate is cut with A_2
- Step 3 The eluate droplet and the spheroid droplet are merged with A_1 and A_2.
- Step 4 The merged droplet is moved to J via A_1.
- Step 5 The merged droplet is mixed in the zigzag flow channel in EC and collected under a negative pressure applied via L_3.

In the experiments in Section III, spheroids of U87 MG (The human glioblastoma U87MG cell line, ATCC, USA) were used and PBS with 5-mol/L NaCl was used for the elute droplet.

F. Visual feedback control

Diluent solutions, such as PBS, are transparent. To detect transparent droplets, we employed the background subtraction method (see the Supplementary Material). The measurement error of the droplet position was ± 2 pixels, ±125 μm in length. Two visual control laws were implemented.
(1) Velocity feedforward control with on–off position control: This control law moved a droplet through feedforward control via an air pump and turned it off when the droplet reached the predetermined position. This control law was used in steps 1–6 and 8 to move a droplet in the binding and washing processes.
(2) Velocity feedback control: In the mixing (step 7) of the washing process, velocity control of a droplet is necessary; hence, the proportional control of the velocity was implemented. The droplet velocity was estimated from its increment during 30 frames, i.e., every 1 s, to reduce noise.

G. Blocking

Blocking treatment is required to prevent the attachment of nonspecific-binding phages in the flow channel. Introducing the blocking liquid into the flow channel, it entered the airflow subchannels and rendered them hydrophilic. This caused problems in droplet transport and the mixing of two droplets. To solve this problem, we prevented the entrance of the air channel from becoming hydrophilic by introducing a blocking liquid as a droplet and passing it in DE at a high flow velocity.

The proposed droplet blocking method is as follows.
- Step 1: Approximately 3-μl blocking liquid (2% Perfect-Block, PB01, MobiTec, Germany) was introduced into the liquid flow channel; this formed a droplet.
- Step 2: The droplet was reciprocated five times at a speed of approximately 6 mm/s in R1 of the flow channel in Fig. 6.
- Step 3: The droplet was passed through DE at a high speed of 12 mm/s and moved into R2.
- Step 4: Step 2 was repeated in R2.
- Step 5: Step 3 was repeated, but the droplet was moved into R1.

Steps 2–5 were repeated for 30 min. Blocking treatment is also performed in EC separately in the same way.

The following experiment was performed to evaluate the droplet blocking method (excluding the blocking treatment in EC):
(1) Three devices were prepared using the same mold.
(2) Normal blocking processing was performed in the first device. This involved the introduction of the blocking liquid into the flow channel of the device entirely. The droplet blocking processing was performed in the second device. The third device was not processed.
(3) The first and second devices were washed using PBS.
(4) A nonspecific-binding phage (T7 phage constructed using the T7 Select 10-3b vector, Merck Millipore, USA) solution (titer: 1.04×10^{10} pfu/mL) was introduced and reciprocated in the entire channel five times at a flow velocity of approximately 6 mm/s.
(5) The channel was filled with the eluate (5-mol/L NaCl solution, Wako, Japan) and let stand for 30 min.
(6) A 250-μL PBS was introduced, and the eluate was recovered.
(7) Plaque assay was performed for the eluate, and the titer was measured (for materials for plaque assay, see the Supplementary Material).

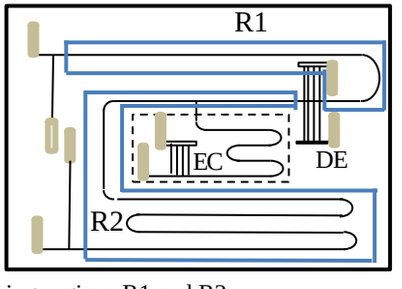

FIG. 6. Blocking regions R1 and R2.

III. Experimental results

A. Visual feedback control

Fig. 7 shows the input–output relationship, where the input is the command value to the air pump, and the output is the average velocity of a droplet. As the air pressure applied to a droplet varies depending on the position of the flow channel, the average velocity was evaluated based on the average of the velocities in the four straight portions of the zigzag flow channel. From Fig. 7, the output average velocity was approximately proportional to the air pump input. Fig. 8 depicts the results of the on–off position control. The target position was at the 466-th pixel, and the steady-state error was 2 pixels (125 μm in length), which is within the target error of 200 μm.

Fig. 9 displays the velocity feedback control results. The desired velocity was 1.06 pixels/frame (2 mm/s). The velocity was oscillatory but controlled within 2 ± 1 mm/s, which was sufficient because the capturing and washing processes required several steps of velocity differences, e.g., low (3 mm/s), lower medium (5 mm/s), higher medium (7 mm/s), and high (9 mm/s) velocities.

B. Operation confirmation

Experiments were performed to confirm that the developed device could perform the proposed operations described in Section II.

(1) Binding and washing processes using colored water:

Blue-dyed water (Food dye blue, Kyoritsu-foods, Japan) was used for a spheroid droplet to visualize the dilution with a transparent diluent solution of PBS (Wako, Japan). Fig. 10 shows images of the device for steps 1–7 of the binding and washing processes, except for step 4 (which is examined in other experiments). EC was not installed in the device for this experiment.

- Step 1: A droplet of blue pure water was introduced into the flow channel manually via S_1.

Then, the control program could perform the following.

- Step 2: The droplet was moved to region DE.
- Step 3: The droplet stayed in region DE during drainage. The initial area of the droplet was 4,096 pixels, and the target area was 400 pixels. The liquid in the droplet was drained, and the area of the droplet was reduced to 416 pixels, (16-pixel (4%) error compared with the target area).
- Step 5: The diluent solution (PBS) was introduced into the flow channel via L_1 and cut to form a droplet via A_2. The dilution ratio was 1:5, and the target area of the droplet was 16 × 5 = 2,080 pixels. The area of the droplet was 2,126 pixels, (46-pixel (2.2%) error compared with the target area). The air between the diluent solution and blue droplet pushed the blue droplet, but it stopped on the right of DE.
- Step 6: Two droplets were merged by exhausting the air between them from DE.
- Step 7: The liquid in the merged droplet was mixed by reciprocating it in the zigzag flow channel.

(2) Eluting/collecting process using transparent solutions:

Fig. 11 shows the experimental result of the eluting/collecting process. A PBS droplet with a spheroid of U87 MG was initially set on the left of DE, which was the drained

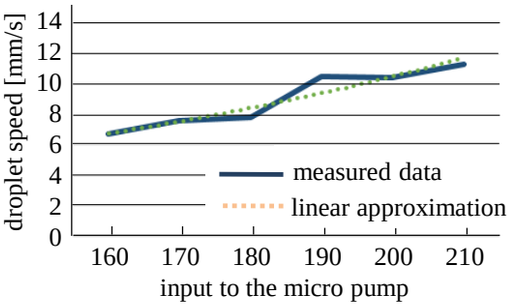

FIG. 7. Relationship between the micropump input and output average velocity

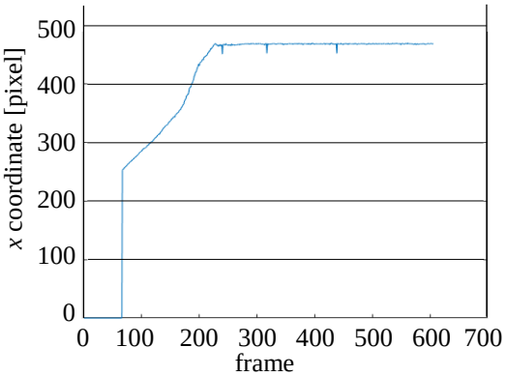

FIG. 8. Result of on–off position control (1 pixel = 62.5 μm, 1 flame = 0.33 s).

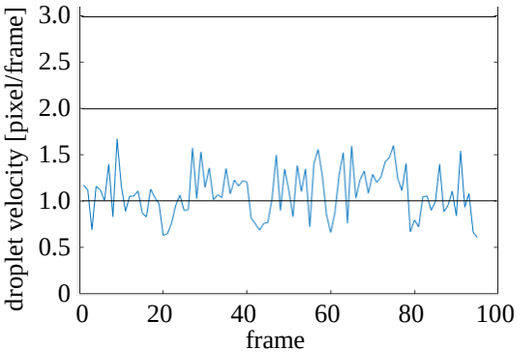

FIG. 9. Results of velocity feedback control of a droplet (1 pixel = 62.5 μm, 1 flame = 0.33 s).

droplet after the washing process described next (see (3)).

- Step 1: A PBS elute droplet was introduced with S_2 and was moved into the main channel via L_3.
- Step 2: The elute droplet was cut with air pressure via A_2.
- Step 3: The two droplets were merged with A_1 and A_2.
- Step 4: The merged droplet was moved to J via A_1.
- Step 5: The merged droplet was collected via L_3.

(3) Binding and washing using transparent solutions:

The binding process and step 4 of the washing process were performed using transparent PBS solutions. See a video in the Supplementary Material. Fig. 12 shows a photo of the droplet containing the U87 MG spheroid. It could transport the spheroid and could pass the junction J. That is, a little part of the droplet entered the branch flow channel and it was brought out by the main volume of the droplet.

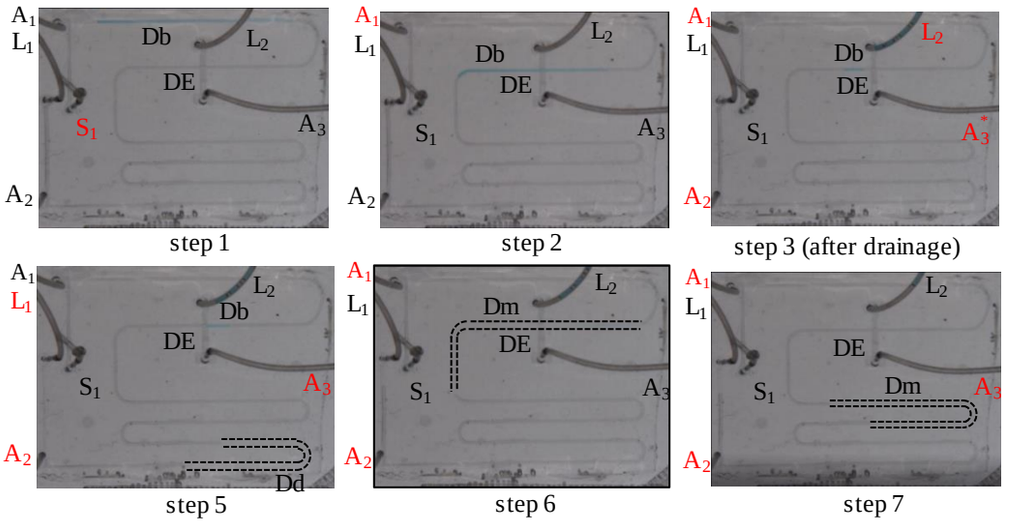

FIG. 10. Experimental results of the binding and washing processes (EC was not installed. Db: droplet of blue-dyed water, Dd: droplet of the diluent solution, and Dm: merged droplet) On pumps are colored red. Step 1: introduction of Db from S_1. Step 2: movement to DE via A_1, Step 3: drainage from L_2, Step 5: introduction of Db from L_1, Step 6: merging of the two droplets, and Step 7: reciprocation of the merged droplet Dm for mixing (A_1 and A_2 are switched on alternatively; when A_1 is on, A_3 is also on).

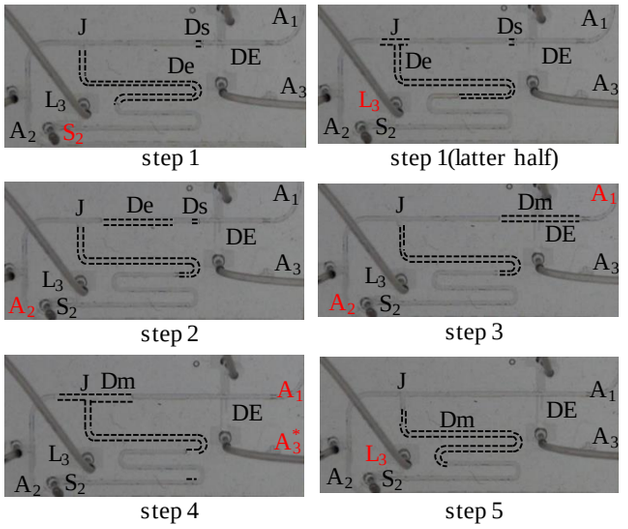

FIG. 11. Eluting/collecting process using transparent solutions(Ds: spheroid droplet, De: elute droplet, and Dm: merged droplet). On pumps are colored red. Step 1: introduction of an elute solution from S_2 and move to the main channel, Step 2: cutting off the elute solution to form the droplet De via A_2, Step 3: merging of the two droplets De and Ds to form Dm, Step 4: movement to J, and Step 5: collection of Dm via L_3.

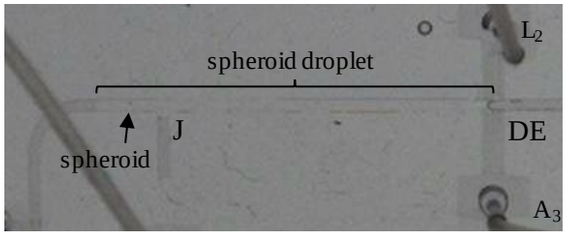

FIG. 12. Photo of a spheroid droplet.

C. Blocking

Table 1 summarizes the results of the phage recovery ratios of normal, droplet, and no-blocking devices. Those of the normal and droplet blocking devices were 10 times smaller than that of the no-blocking device. The effect of the droplet blocking method was almost the same as that of the normal blocking.

D. Washing experiment using phage

We evaluated the washing performance including step 4 of flush washing using the nonspecific-binding phage. Table 2 lists the values of the parameters in the binding and washing processes described in Subection II-D. A U87MG spheroid with a diameter of approximately 300 μm was introduced in step 1. In step 3, the drained liquid was collected in each iteration of the process, and plaque assay was applied to each collected liquid. Iteration 0 means the collection of the drained liquid after the binding process in step 2. Table 3 shows the results. After three iterations, it was confirmed that the reduction ratio was on the order of 10^{-3}.

Table 1. Results of the blocking evaluation experiments.

Recovery ratio	Normal blocking	Droplet blocking	No blocking
1	0.25%	0.61 %	8.76 %
2	0.25%	0.34 %	5.32 %
3	0.12%	0.44 %	6.60 %
Average	0.20%	0.46 %	6.89 %

Table 2. Values of the parameters in the binding and washing processes.

Step	Parameter	Value
2	Target speed of droplet	3 mm/s
3	Target area of droplet liquid after drainage	200 pixels
4	Volume of flush liquid	30 μL
5	Ratio of dilution	1:5
7	Number of reciprocation and target speed of droplet	5 and 6 mm/s

Table 3. Experimental results of washing.

Iteration	First [pfu]	Second [pfu]	Third [pfu]
0	7.46×10^5	8.76×10^5	2.34×10^5
1	3.51×10^4	1.58×10^4	2.54×10^4
2	4.63×10^3	5.44×10^3	2.97×10^3
3	7.56×10^2	7.44×10^2	5.28×10^2
Ratio of 3 to 0	1.01×10^{-3}	0.85×10^{-3}	2.26×10^{-3}

IV. Discussion

In this article, we proposed a microfluidic system that has functions to perform phage-display screening against spheroids, which is a necessary step toward the goal of phage-display screening against spheroids. We should address what remains to be done to achieve this goal.

(1) Efficient, concise, and reliable phage quantifying method: Phage-display screening requires quantifying phages many times[7]. Plaque assay, the most typical method of quantifying phages, is time-consuming and requires technical proficiency (e.g., careful *E. coli* culture) to be reliable, making it difficult to perform phage-display screening. An alternative method that can quantify phages more efficiently and concisely is highly desired. Phage quantifying methods based on fluorescence staining of phages that achieved a sufficient detection limit have been proposed[23,24]. We will apply such a method to quantify phages binding to spheroid cells.

(2) Known proteins or peptides that can specifically bind to spheroid cells: For efficient screening, it is necessary to optimize the flow rate for binding, which maximizes phages that can specifically bind to spheroid cells, and the flow rate for washing, which maximizes the ratio of specific and nonspecific-binding phages. Known proteins or peptides that can specifically bind to spheroid cells are necessary for these optimizations. However, because the status of surface proteins of the monolayer cultured cells is not necessarily the same as that of 3D cultured cells, specific binding phages to monolayer cultured cells may not be specific binding ones to spheroid cells. We should carefully investigate the differences of specific binding phages with a reliable phage quantifying method.

(3) Uniform formation of spheroids: To perform comparative experiments, it is also necessary to make the sizes of spheroids as uniform as possible.

The following limitations of the current system should also be addressed.

(1) The spheroid is not easily introduced into the microchannel.

Currently, a spheroid from a 96-well plate is manually introduced into the microchannel using a syringe. This transfer requires skill and can transfer only one spheroid into one droplet. Kim et al.[25] proposed a contact-based spheroid transfer method that can transfer spheroids formed by the conventional hanging drop method to another device. This method proved useful in drug transfer because it can be performed in stationary droplets. However, the binding, washing, and eluting of phage-display screening, which are difficult to perform in stationary droplets, can be achieved in moving droplets (as demonstrated in the proposed microfluidic device). The contact-based spheroid transfer method cannot be applied to the proposed microfluidic device. Automatic transfer of spheroid into the proposed microfluidic device could be achieved by integrating the droplet-based spheroid formation method[26]

(2) The clarity of the spheroid image should be improved.

Although the camera used in the present system detected the droplets, the images of an introduced spheroid were unclear and not detectable using computational image processing. Currently, the operator must visually monitor the video of the moving spheroid droplet. If the spheroid is left behind the droplet, the operator can retrieve the spheroid by halting the running program; that is, by manually moving the droplet back to the spheroid using the syringe pumps. The program is then resumed. This manual recovery operation impairs the degree of automation. A higher speed and resolution camera might resolve this problem. Fluorescent imaging can more reliably detect a spheroid than camera imaging, but requires a fluorescent microscope and possibly an electric xy-stage to cover the whole microfluidic device. Computer control of the stage is also required to follow the spheroid droplet.

(3) Endocytosis must be suppressed in the system.

When targeting a live spheroid rather than a formalin-fixed spheroid, endocytosis must be suppressed by maintaining the device at 4°C. In future work, we will design and develop a system that can function at 4°C.

(4) Limitations of spheroids

The advantages of spheroids over monolayer cell culture were mentioned in Section I. However, spheroids are cell aggregations with no organic structure. Recently, organ-on-a-chips and organoids have been attracting interest[27] as ex-vivo cell models that can imitate organ functions and patient-specific diseases. Phage-display screening using such excellent ex-vivo cell models is an important direction of the present study.

V. Conclusions

In this study, we proposed a valveless droplet-based microfluidic system for phage-display screening against spheroids using a camera, three liquid pumps, and three air pumps. We experimentally verified that the system could detect and actively control droplets and that it could perform the binding, washing, eluting, and collecting processes of phage-display screening with the proposed operation sequences. In addition, we evaluated the performance of the proposed blocking method and flush washing with plaque assay using phages.

Finally, we discussed our perspective to achieve the goal of phage-display screening against spheroids and the limitations of the proposed system.

SUPPLEMENTARY MATERIAL

See the Supplementary Material for the fabrication process, background subtraction method, materials for plaque assay, and video of the experiment of binding and washing processes using transparent solutions.

AUTHORS' CONTRIBUTIONS

T. S. and A. H. developed the system and performed the experiments. T. K. and S. K-K. participated in the discussion from the biology point of view. T. O supervised the research and wrote the manuscript.

ACKNOWLEDGMENTS

We would like to thank Prof. Tadashi Ishida for his useful inputs. This work was supported by JPSP KAKENHI grant numbers 16H02320 and 20H00228, and the Mechano Micro Processing Laboratory of Tokyo Institute of Technology.

There are no conflicts of interest to declare.

DATA AVAILABILITY

The data that support the findings of this study are available from the corresponding author upon reasonable request.

REFERENCES

[1]G. P. Smith, "Filamentous Fusion Phage: Novel Expression Vectors That Display Cloned Antigens on the Virion Surface," Science, 228, 1315-1317 (1985).
[2]C. D. Barbosa, M. D. M. Brigido, and A. Q. Maranhao, "Antibody Phage Display Libraries: Contributions to Oncology," Int. J. Mol. Sci. 13, 5420-5440 (2012).
[3]S. H. White, W. C. Wimley, "Membrane protein folding and stability: Physical principles," Annu. Rev. Biophys. Biomol. Struct. 28, 319-365 (1999).
[4]J. E. Butler, P. Navarro, and J. Sun, "Adsorption-induced antigenic changes and their significance in ELISA and immunological disorders," Immunol. Invest. 26, 39-54 (1997).
[5]J. E. Butler, L. Ni, R. Nessler, K. S. Joshi, M. Suter, B. Rosenberg, J. Chang, W. R. Brown, and L. A. Cantarero, "The physical and functional behavior of capture antibodies adsorbed on polystyrene," J. Immunol. Methods, 150, 77-90 (1992).
[6]M. A. Alfaleh, M. L. Jones, C. B. Howard, and S. M. Mahler, "Strategies for selecting membrane protein-specific antibodies using phage display with cell-based panning," Antibodies 6 (2017).
[7]J. Wang, Y. Liu, T. Teesalu, K. N. Sugahara, V. R. Kotamrajua, J. D. Adams, B. S. Ferguson, Q. Gong, S. S. Oh, A. T. Csordas, M. Cho, E. Ruoslahti, Y. Xiao, and H. T. Soh, "Selection of phage-displayed peptides on live adherent cells in microfluidic channels," Proc. Natl. Acad. Sci. USA, 108, 6909-6914 (2011).
[8]C.-H. Wang, C.-H. Weng, Y.-J. Che, K. Wang, and G.-B. Lee, "Cancer Cell-Specific Oligopeptides Selected by an Integrated Microfluidic System from a Phage Display Library for Ovarian Cancer Diagnosis," Theranostics, 5, 431-442 (2015).
[9]Y.-J. Che, H.-W. Wu, L.-Y, Hung, C.-A. Liu, H.-Y. Chang, K. Wang, and G.-B. Lee, "An integrated microfluidic system for screening of phage-displayed peptides specific to colon cancer cells and colon cancer stem cells," Biomicrofluidics, 9 (2015).
[10]B. H. Gorden, J.-H. Kim, A. L. Sarver, A. M. Frantz, M. Breen, K. L. Toh, T. D. O'Brien, L. C. Sharkey, J. F. Modiano, E. B. Dickerson, "Identification of three molecular and functional subtypes in canine hemangiosarcoma through gene expression profiling and progenitor cell characterization," Am. J. Pathol. 184, 985-995 (2014).
[11]L. Gaedtke, L. Thoenes, C. Culmsee, B. Mayer, and E. Wagner, "Proteomic Analysis Reveals Differences in Protein Expression in Spheroid versus Monolayer Cultures of Low-Passage Colon Carcinoma Cells," J. Proteome Res. 6, 4111-4118 (2007).
[12]K. Moshksayana, N. Kashaninejadb, M. E. Wrkianic, J. G. Lock, H. Moghadas, B. Firoozabadi, M. S. Saidi, N.-T. Ngyuen, "Spheroids-on-a-chip: Recent advances and design considerations in microfluidic platforms for spheroid formation and culture," Sens. Actuators B: Chem., 263, 151-176 (2018).
[13]T. Ishida, K. Ikeda, and T. Omata, In-droplet peptide screening microfluidic device targeting cancer cell spheroids, 22nd Int. Conf. on Mniaturized Systems for Chemistry and Life Sciences, 1125-1127 (2018).
[14]A. Hamai, T. Ishida, and T. Omata, "Automation of screening device for cancer cell-specific binding peptides using spheroids," Proc. of JSME Conf. on Robotics and Mechatronics, Japan, 2P1-F06 (2019) (in Japanese).
[15]T. Sato and T. Omata, "Automation device for cancer cell-binding peptide screening using spheroids - design and automation of elution process -," Proc. of the 2020 JSME Conf. on Robotics and Mechatronics, 2P1-O05 (2020) (in Japanese).
[16] S.-Y. Teh, R. Lin, L.-H. Hung, and A. P. Lee, "Droplet microfluidics," Lab. Chip, 8, 198-220 (2008).
[17]M. T. Guo, A. Rotem, J. A. Heymana, and D. A. Weitz, "Droplet microfluidics for high-throughput biological assays," Lab. Chip, 12, 2146-2155 (2012).
[18]F. Sarrazin, L. Prat, N. D. Miceli, G. Cristobal, D. R. Link, and D. A. Weitz, "Mixing characterization inside microdroplets engineered on a microcoalescer," Chem. Eng. Sci. 62, 1042-1048 (2007).
[19]T. Ishida, D. McLaughlin, Y. Tanaka, T. Omata, "First-come-first-store microfluidic device of droplets using hydrophobic passive microvalves," Sens. Actuators B Chem. 254, 1005-1010 (2018).
[20] H.-D. Xi, H. Zheng, W. Guo, A. M. G.-Calvo, Y. Ai, C.-W. Tsao, J. Zhou, W. Li, Y. Huang, N.-T. Nguyen, S. H. Tan, "Active droplet sorting in microfluidics: a review," Lab. Chip, 17, 751-771 (2017).
[21]M. Hébert, M. Courtney, and C. L. Ren, "Semi-automated on-demand control of individual droplets with a sample application to a drug screening assay," Lab. Chip, 19, 1490-1501 (2019).
[22]M. Kaminaga, T. Ishida, and T. Omata, "Microvalve with Trapezoid-Shaped Cross-Section for Deep Microchannels," micromachines, 12 (2021).
[23]J.-H. Han, M. S. Wang, J. Das, L. Sudheendra, E. Vonasek, N. Nitin, and I. M. Kennedy, "Capture and Detection of T7 Bacteriophages on a Nanostructured Interface," ACS Appl. Mater. Interfaces 6, 4758-4765 (2014).
[24]R. Edgar, M. McKinstry, J. Hwang, A. B. Oppenhei, R. A. Fekete, G. Giulian, C. Merril, K. Nagashima, and S. Adhya, "High-sensitivity bacterial detection using biotin-tagged phage and quantum-dot nanocomplexes," PNAS, 103, 4841-4845 (2006).
[25]H. Kim, C. H. Cho, and J.-K. Park, "High-throughput culture and embedment of spheroid array using droplet contact-based spheroid transfer," Biomicrofluidics 12, (2018)
[26]J. M. Lee, J. W. Choi, C. D. Ahrberg, H. W. Choi, J. H. Ha, S. G. Mun, S. J. Mo and B. G. Chung, "Generation of tumor spheroids using a droplet-based microfluidic device for photothermal therapy," Microsyst. Nanoeng., 6 (2020).
[27]D. Huang , X. Zhang, X. Fu, Y. Zu, W. Sun, and Y. Zhao, "Liver spheroids on chips as emerging platforms for drug screening," Engineered Regeneration 2, 246-256 (2021).

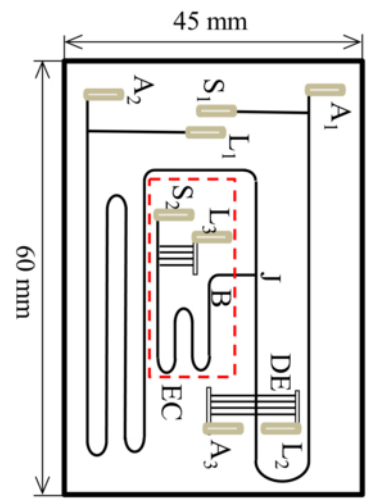

PLEASE CITE THIS ARTICLE AS DOI: 10.1063/5.0085459

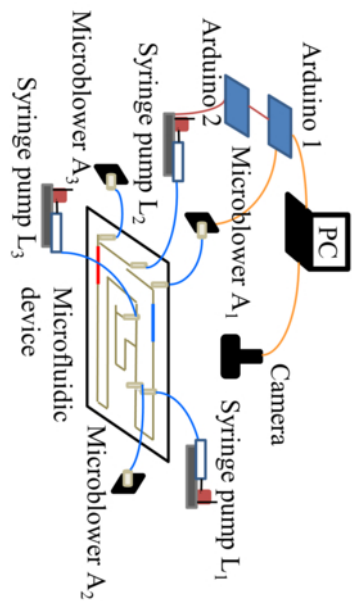

AIP Publishing

Biomicrofluidics

ACCEPTED MANUSCRIPT

PLEASE CITE THIS ARTICLE AS DOI: 10.1063/5.0085459

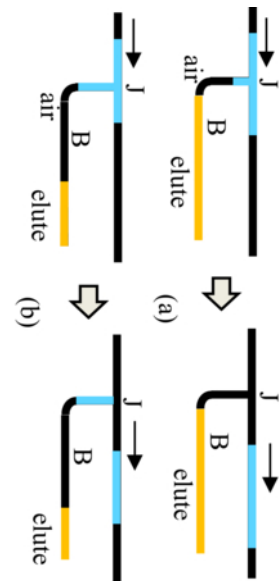

Biomicrofluidics

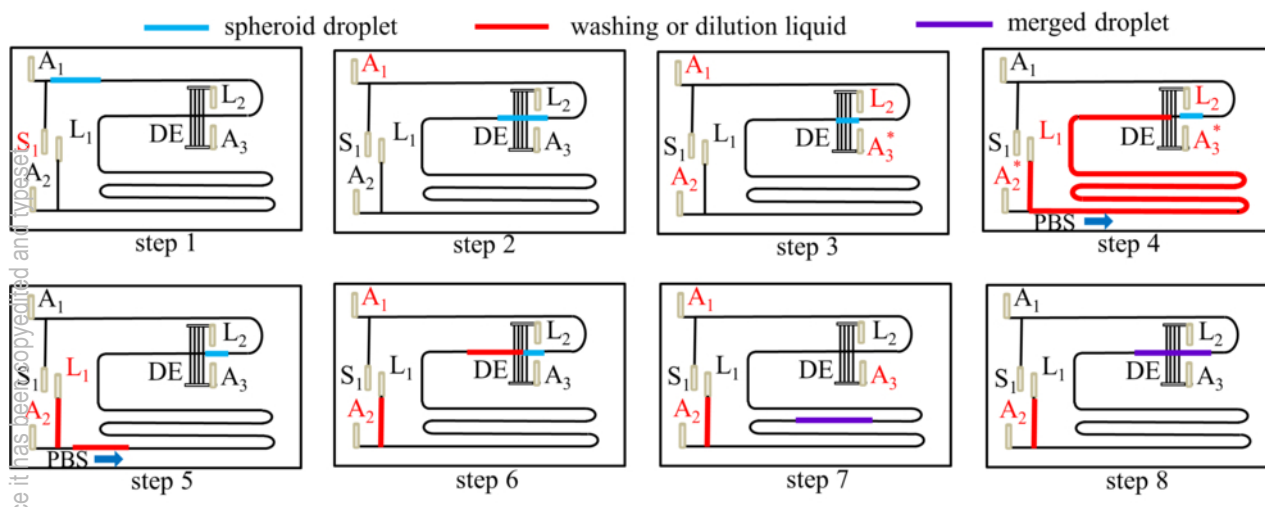

AIP Publishing

Biomicrofluidics

ACCEPTED MANUSCRIPT

This is the author's peer reviewed, accepted manuscript. However, the online version of record will be different from this version once it has been copyedited and typeset.
PLEASE CITE THIS ARTICLE AS DOI: 10.1063/5.0085459

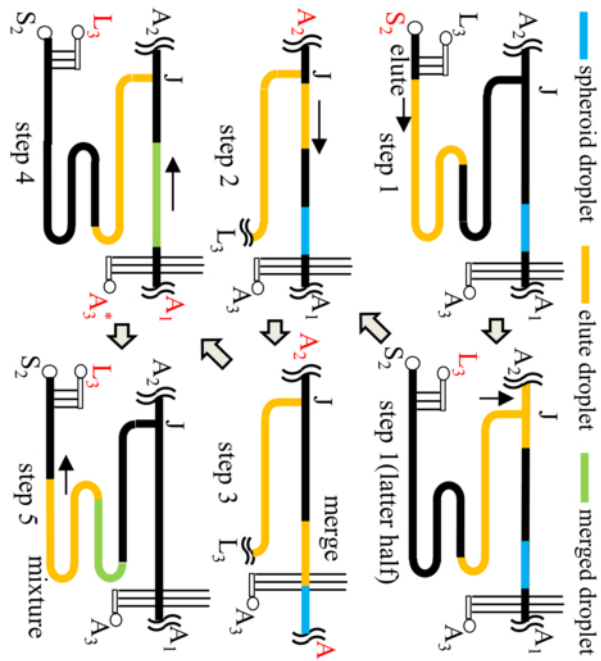

Biomicrofluidics

PLEASE CITE THIS ARTICLE AS DOI: 10.1063/5.0085459

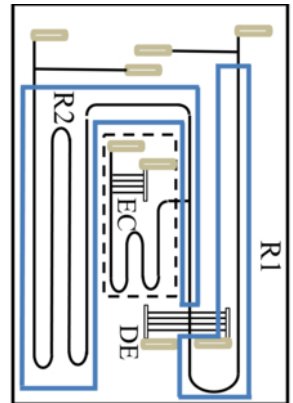

AIP Publishing

Biomicrofluidics

ACCEPTED MANUSCRIPT

PLEASE CITE THIS ARTICLE AS DOI: 10.1063/5.0085459

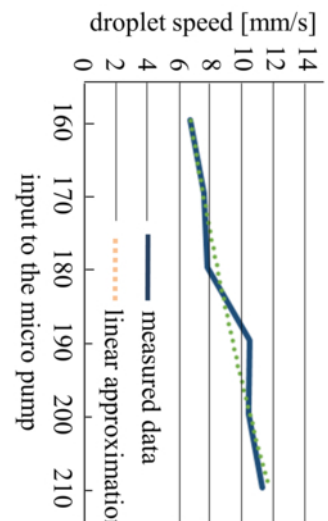

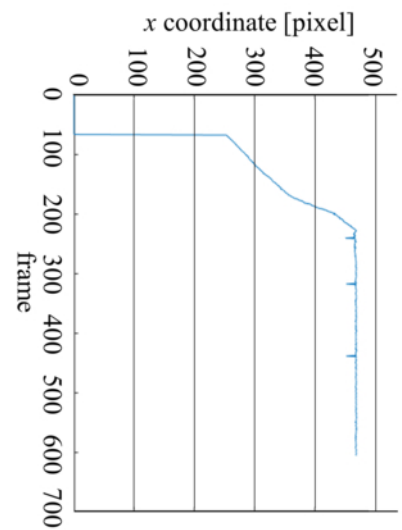

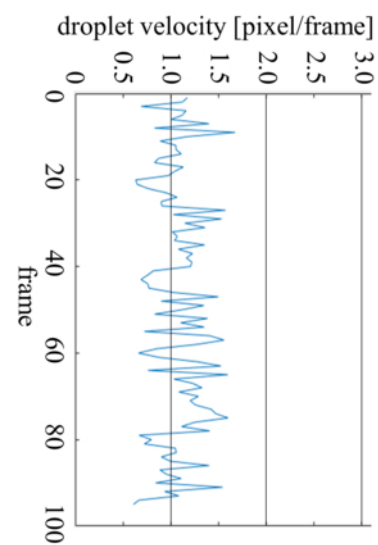

Biomicrofluidics

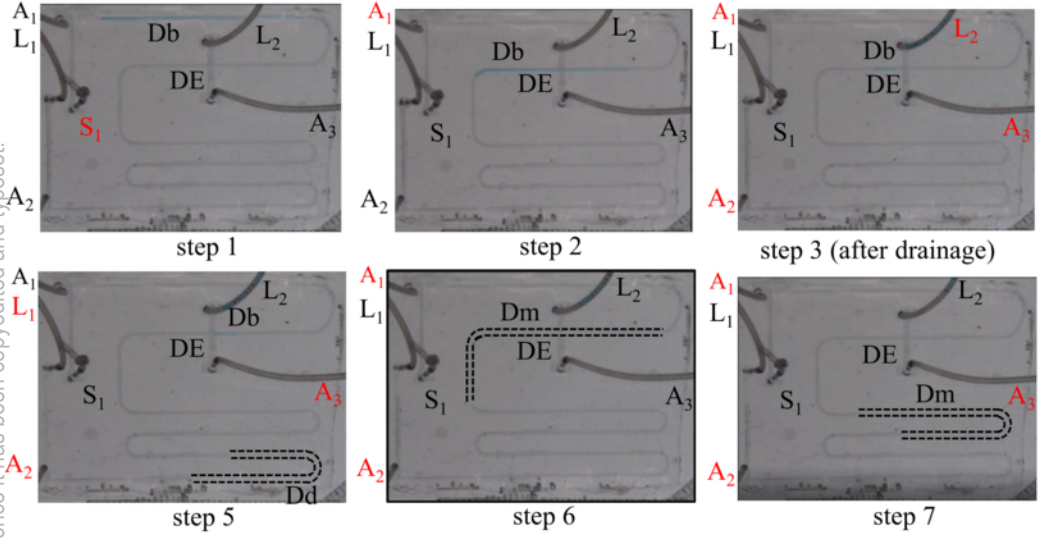

AIP Publishing

Biomicrofluidics

ACCEPTED MANUSCRIPT

PLEASE CITE THIS ARTICLE AS DOI: 10.1063/5.0085459